Nigerian Journal of Technology (NIJOTECH)
Vol. 32. No. 2. July 2013, pp. 304 – 317

University of Nigeria, Nsukka, ISSN 1115-8443
www.nijotech.com

AN IMPROVED VOLTAGE REGULATION OF A DISTRIBUTION NETWORK USING FACTS - DEVICES

O. T. Onyia, T. C. Madueme, C. O. Omeje
DEPARTMENT OF ELECTRICAL ENGINEERING, UNIVERSITY OF NIGERIA, NSUKKA
E-mail: osmond4us@yahoo.com, theophilus.madueme@unn.edu.ng, omejecrescent@yahoo.com

Abstract
This paper comparatively explored the power quality of a thirteen bus, 33/11kv distribution network. The analysis of this network was actualized using the conventional load flow equation modeling. In furtherance to the mathematical modeling of the network analysis was the incorporation of a Static Compensator (STATCOM), a Flexible Alternating Current Transmission System Device which is power electronic-controlled on the specified bus under study. The Newton-Raphson Load flow equation modeling was a veritable tool applied in this analysis to determine the convergence points for the voltage magnitude, power (load) angle, power losses along the lines, sending end and receiving end power values at the various buses that make up the thirteen bus network. The graphical representations of the iteration results obtained from Newton-Raphson load flow analysis were presented to show the effects of injecting a Flexible Alternating Current Transmission System Device on the power line over the generally known conventional technique that employs electromechanical concepts.

***Keywords*:** Facts-Devices, Power Flow Analysis and Newton Raphson Iteration Algorithm.

Abbreviations:
STATCOM: Static Compensator
FACTS-DEVICE: Flexible Alternating Current Transmission System Device
HVDC: High Voltage Direct Current
TCR: Thyristor-Controlled Reactor
SVC: Static Var Compensator
TCSC: Thyristor Controlled Series Compensator
THD: Total harmonic distortion
VSC: Voltage Source Converter
A.C: Alternating Current
VAR: Volts Ampere Reactive

1. Introduction

A flexible alternating-current transmission system (FACTS) is a recent technological development in electrical power systems. It is built on the great many advances achieved in high-current, high-power semiconductor devices technology. From the power systems engineering perspective, the applications of these emerging power electronic equipment and techniques as a means of alleviating long-standing operational problems in both high-voltage transmission and low-voltage distribution systems have contributed significantly to the rapid advancement in maintaining the voltage and power limits of the specified network within a prescribed magnitude.

FACTS devices are used to achieve several goals. They can permit the operation of transmission/distribution lines close to their thermal limits and also reduce the loop flows. In this respect, they act by supplying or absorbing reactive power, increasing or reducing voltage magnitude and controlling series impedance or phase angle. They are also capable of increasing synchronizing torque, damp oscillation at various frequencies below/above the rated frequency

value, thus supporting dynamic voltage or control power flows.

2. Facts controllers based on conventional thyristors

Power electronic circuits using conventional thyristors have been widely used in power transmission applications in the early 1970s [1]. The first applications took place in the area of HVDC transmission. More recently, fast-acting series compensators using thyristors have been used to vary the electrical length of key transmission lines, with a reduced delay, instead of the classical series capacitor which is mechanically controlled. In distribution system applications, solid state transfer switches using thyristors are being used to enhance the reliability of supply to critical customer loads [1]. In this section, the following three thyristor-based controllers are analyzed: TCR, SVC and TCSC.

2.1 The thyristor-controlled reactor

The main components of the basic TCR are shown in figure 1. The controllable element is the anti-parallel thyristor pair, TH1 and TH2, which conducts on alternate half-cycles of the supply frequency. The other key component is the linear (air core) reactor of inductance L. The overall action of the thyristor controller on the linear reactor is to enable the reactor to act as a controllable susceptance, in the inductive sense, which is a function of the firing angle α. However, this action is not trouble free, since the TCR achieves its fundamental frequency steady-state operating point at the expense of generating harmonic distortion, except for full conduction. The reactor contains little resistance and the current is essentially sinusoidal and inductive, lagging the voltage by $90^0\left(\frac{\pi}{2}\right)$ .The relationship between the firing angle α of the thyristor and the corresponding conduction angle δ is derived from (1)

$$\delta = 2(\pi - \alpha) \quad (1)$$

Partial Conduction is achieved with firing angles in the range $\frac{\pi}{2} < \alpha < \pi$ in radians. Increasing the value of firing angle above $\frac{\pi}{2}$ causes the TCR current waveform to become non-sinusoidal, with its fundamental frequency component reduced in magnitude. This, in turn, is equivalent to an increase in the inductance of the reactor thus reducing its ability to draw reactive power from the network at the point of connection [2].

2.2 The static var compensator

In its simplest form, the SVC consists of a TCR in parallel with a bank of capacitors. From an operational point of view, SVC behaves like a shunt-connected variable reactance, which either generates or absorbs reactive power in order to regulate the voltage magnitude at the point of connection to the AC network. It is used extensively to provide fast reactive power and voltage regulation support. The firing angle control of the thyristor enables SVC to have almost instantaneous speed of response

A schematic representation of the SVC is shown in figure 2, where a three-phase, three winding transformer is used to interface the SVC to a high-voltage bus.

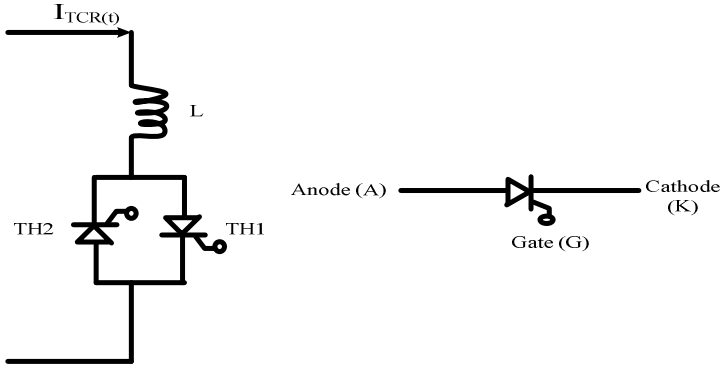

Figure 1: Basic thyristor controlled reactor and thyristor circuit symbol

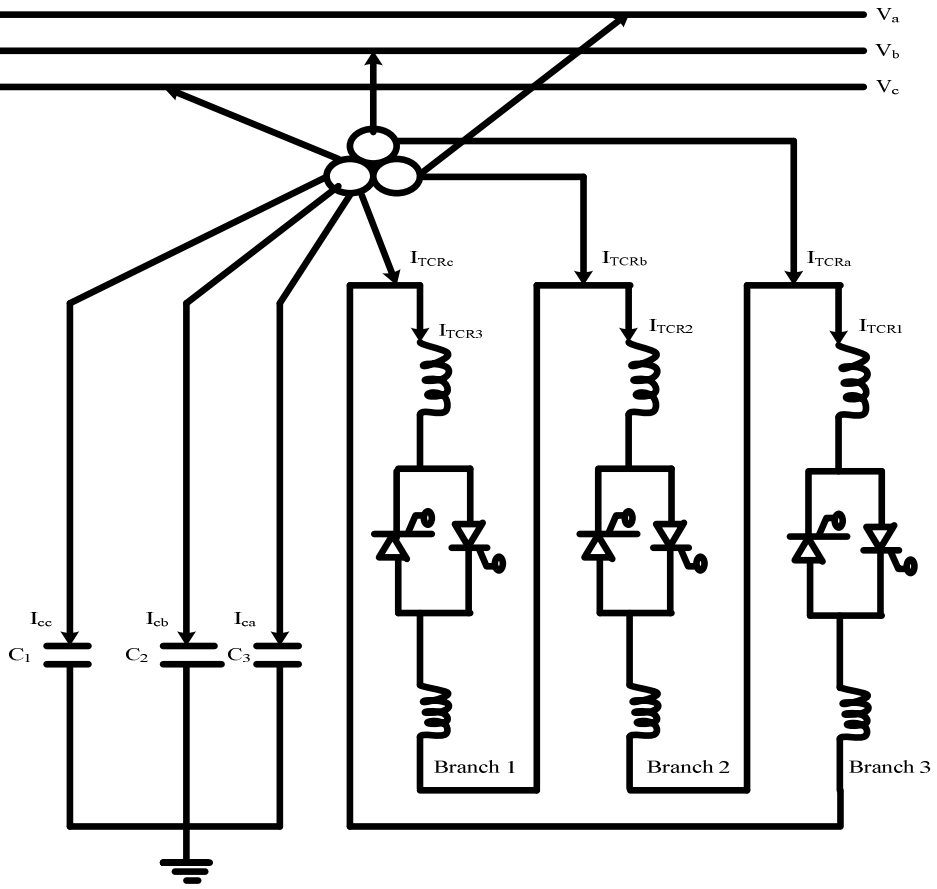

Figure 2. Three Phase Static Var Compensator with Fixed Capacitors and Thyristor Controlled Reactor.

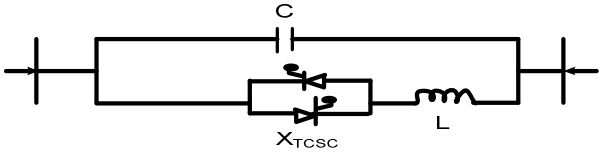

Figure 3: Single phase thyristor controlled series compensator

The transformer has two identical secondary windings: one is used for the delta-connected, Six-pulse TCR and the other for the star-connected, three-phase bank of capacitors, with its star point floating. The three transformer windings are also taken to be star-connected, with their star points floating [3].

2.2.1 The thyristor-controlled series compensator.

TCSCs vary the electrical length of the compensated transmission line with little delay. This characteristic enables the TCSC to be used to provide fast active power flow regulation. It also increases the stability margin of the system and has proved very effective in damping SSR and power oscillations [4].

A basic TCSC module consists of a TCR in parallel with a fix capacitor as shown in figure 3 below.

The TCR achieves its fundamental frequency operating state at the expense of generating harmonic current which depends on the thyristor conduction angle. The TCR harmonic currents are trapped inside the TCSCs because of the low network equivalent impedance. This holds for a well-designed TCSC operating in capacitive mode. Measurements conducted in the Slatt and the Kayenta TCSC systems support this observation. For instance, the Kayenta system generates at its terminals, a maximum THD

voltage of 1.5% when operated in capacitive mode and firing at an angle of 147^0[4]. Little Progress is sparingly made for operating the TCSC in inductive mode as this would increase the electrical length of the compensated power line, with adverse consequences on stability margins, and extra losses [4].

2.3 Principles of voltage source converter operation

The interaction between the (VSC) and the power system may be explained in simple terms, by considering a VSC connected to the **a.c** mains through a loss-less reactor as illustrated in the single-line diagram shown in figure 4a. The voltage at the supply bus is taken to be sinusoidal of value $V_S\langle 0^{0(1)}$ and the fundamental frequency component of the SVC a.c voltage is taken to be $V_{VR}\langle\delta_{VR}$. The positive sequence fundamental frequency vector representation is shown in figures 4b and 4c for leading and lagging VAR compensation respectively. According to figure 4 for both leading and lagging VAR, the active and the reactive powers can be expressed as shown in (2a) and (2b).

$$\mathbf{P} = \frac{\mathbf{V_S \times V_{VR} \sin \delta_{VR}}}{\mathbf{X_L}} \qquad (2a)$$

$$\mathbf{Q} = \frac{\mathbf{V_S^2}}{\mathbf{X_L}} - \frac{\mathbf{V_S \times V_{VR} \cos \delta_{VR}}}{\mathbf{X_L}} \qquad (2b)$$

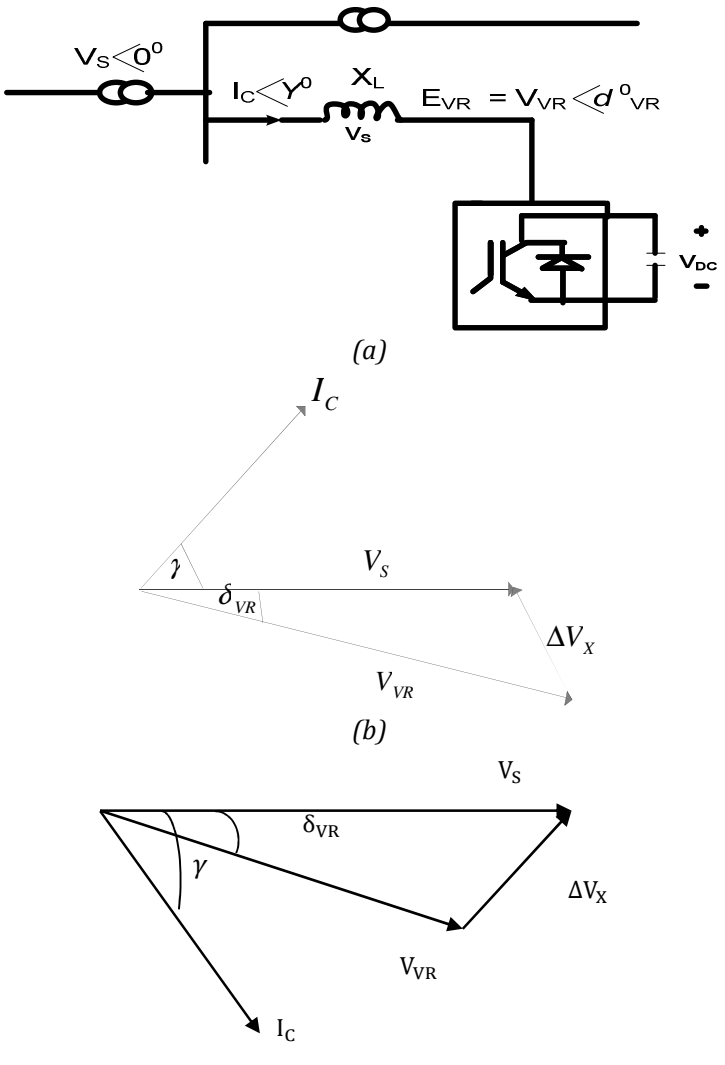

Figure 4: (a) VSC connected to a system bus. (b) lagging operation of the voltage (c) leading operation of the voltage.

With reference to figures 4a, b and c (2a) and (2b), the following observations are derived:

- The VSC output voltage V_{VR} lags the **a.c** voltage source V_S by an angle δ_{VR}, and the input current lags the voltage drop across the reactor ΔV_X by $\frac{\pi}{2}$;
- The active power flow between the **a.c** source and the VSC is controlled by the phase angleδ_{VR}. Active power flows into the VSC from the **a.c** source for lagging δ_{VR} ($\delta_{VR} > 0$) and flows out of the VSC from the Ac source for leading $\delta_{VR}(\delta_{VR} < 0)$;
- The reactive power flow is determined mainly by the magnitude of the voltage source, V_s and the VSC output fundamental voltage, V_{VR} . For $V_{VR} > V_S$, the VSC generates reactive power and consumes reactive power when $V_{VR} < V_S$.

The Dc capacitor voltage V_{DC} is controlled by adjusting the active power flow that goes into the VSC. During normal operations, a small amount of active power must flow into the VSC to compensate for the power losses inside the VSC, and δ_{VR} is kept slightly larger than 0^0 (lagging).

3.0 Mathematical models of conventional and facts controller (statcom) power flow.

For the purpose of steady-state network assessment, power flow solutions are probably the most popular form of computer-based algorithm carried out by planning and operation engineers. Many calculation methods have been put forward to solve this problem. Among them, Newton-Raphson methods, with their strong convergence characteristics have proved the most successful and have been embraced by power industry [5-6]. This paper employed an elegant method for accommodating models of controllable equipment namely STATCOM Flexible Alternating Current Transmission System controller into the Newton-Raphson power flow algorithms.

3.1 Basic equation formulation.

Assuming at a given bus the generation, load, and power exchanged through the transmission elements connecting to the bus add up to zero. Then (3) and (4) are formed.

$$\Delta P_K = P_{GK} - P_{LK} - P_K^{cal} = P_K^{sch} - P_K^{cal} = 0 \quad (3)$$

$$\Delta Q_K = Q_{GK} - Q_{LK} - Q_K^{cal} = Q_K^{sch} - Q_K^{cal} = 0 \quad (4)$$

The terms ΔP_K and ΔQ_K are the active and reactive powers mismatch at bus k while, P_{GK} and Q_{GK} are the active and reactive powers injected by the generator at bus K. P_{LK} and Q_{LK} represent the active and reactive powers drawn by the load at bus K, respectively. In principle, the generation and the load at bus K may be measured by the electric utility while their net values are known as the scheduled active and reactive powers.

$$P_K^{sch} = P_{GK} - P_{LK} \quad (5)$$

$$Q_K^{sch} = Q_{GK} - Q_{LK} \quad (6)$$

The transmitted active and reactive powers, P_K^{cal} and Q_K^{cal} , are functions of nodal voltages and network impedances and are computed using the power flow equations.

However, if the nodal voltages are not known precisely then the calculated transmitted powers will have only approximated values and the corresponding mismatch powers are not zero.

In modern power flow computer programs, it is normal for all mismatch equations to satisfy a tolerance as tight as e^{-12} before the iterative solution can be considered successful. In order to develop suitable power flow equations, it is expedient to derive a relational equation between injected bus currents and bus voltages.

Based on figure 5 the injected complex current at bus K, denoted by I_K , may be expressed in terms of the complex bus voltages E_K and E_M as presented in (7).

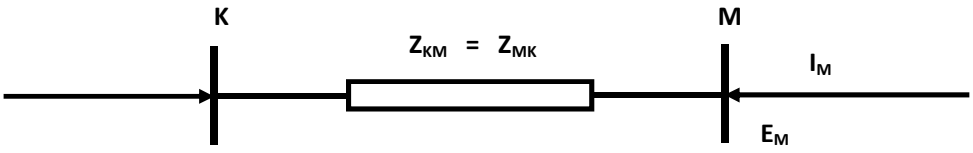

Figure 5: Equivalent Impedance

$$I_K = \frac{1}{Z_{KM}} \times (E_K - E_M) = y_{KM} \times (E_K - E_M) \quad (7)$$

Similarly, for bus M,

$$I_M = \frac{1}{Z_{MK}} \times (E_M - E_K) = y_{MK} \times (E_M - E_K) \quad (8)$$

(7) and (8) can be written in matrix form as shown in (9):

$$\begin{bmatrix} I_K \\ I_M \end{bmatrix} = \begin{bmatrix} y_{km} & -y_{km} \\ -y_{mk} & y_{mk} \end{bmatrix} \times \begin{bmatrix} E_K \\ E_M \end{bmatrix} \quad (9)$$

In compact form, (9.0) is re-written as (10).

$$\begin{bmatrix} I_K \\ I_M \end{bmatrix} = \begin{bmatrix} Y_{KK} & Y_{KM} \\ Y_{MK} & Y_{MM} \end{bmatrix} \times \begin{bmatrix} E_K \\ E_M \end{bmatrix} \quad (10)$$

The bus admittances and voltages can be expressed in more explicit form in (11) & (12).

$$Y_{ij} = G_{ij} + jB_{ij} \quad (11)$$

$$E_i = V_i e^{-J\theta_i} = V_i(\cos\theta_i + j\sin\theta_i) \quad (12)$$

Where i = k, m and j = k, m.

The complex power injected at bus K consists of an active and reactive component and may be expressed as a function of the nodal voltages and the injected current at the bus:

$$S_K = P_K + jQ_K = E_K I_K^* = E_K(Y_{KK}E_K + Y_{KM}E_M)^* \quad (13)$$

Where I_K^* is the complex conjugate of the current injected at bus K.

P_K^{cal} and Q_K^{cal} can be determined by substituting (11) & (12) into (13) and separating them into real and imaginary parts to produce (14) & (15).

$$P_K^{cal} = V_k^2 G_{kk} + V_K V_M[G_{KM}\cos(\theta_K - \theta_M) + B_{KM}\sin(\theta_K - \theta_m)] \quad (14)$$

$$Q_K^{cal} = -V_K^2 B_{KK} + V_K V_M[G_{KM}\sin(\theta_K - \theta_M) - B_{KM}\cos(\theta_K - \theta_M)] \quad (15)$$

Substituting (14) & (15) into (3.0) & (4.0) give rise to (16) & (17).

$$\Delta P_K = P_{GK} - P_{LK} - \{V_k^2 G_{kk} + V_K V_M[G_{KM}\cos(\theta_K - \theta_M) + B_{KM}\sin(\theta_K - \theta_m)]\} \quad (16)$$

$$\Delta Q_K = Q_{GK} - Q_{LK} - \{-V_k^2 B_{kk} + V_K V_M[G_{KM}\sin(\theta_K - \theta_M) - B_{KM}\cos(\theta_K - \theta_m)]\} \quad (17)$$

Similar equations may be obtained for bus M by simply exchanging subscripts K with M in (16) and (17). For numerous buses and transmission elements, (14) and (15) are expressed in more general term as presented in (18) & (19)

$$P_K^{cal} = \sum_{i=1}^{n} P_K^{ical} \quad (18)$$

$$Q_K^{cal} = \sum_{i=1}^{n} Q_K^{ical} \quad (19)$$

Substituting (18) & (19) into (3.0) & (4.0) give rise to (20) & (21) respectively.

$$\Delta P_K = P_{GK} - P_{LK} - \sum_{i=1}^{n} P_K^{ical} = 0 \quad (20)$$

$$\Delta Q_K = Q_{GK} - Q_{LK} - \sum_{i=1}^{n} Q_K^{ical} = 0 \quad (21)$$

3.2 The newton-raphson power flow model

In large-scale power flow studies the Newton-Raphson method has proved most successful owing to its strong convergence characteristics. This approach uses iteration to solve the following set of nonlinear algebraic equations presented in (22) [7-10].

$$F_1(X_1, X_2, \cdots X_N) = 0; F_2(X_1, X_2, \cdots X_N) = 0; F_3(X_1, X_2, \cdots X_N) = 0; F(X) = 0 \quad (22)$$

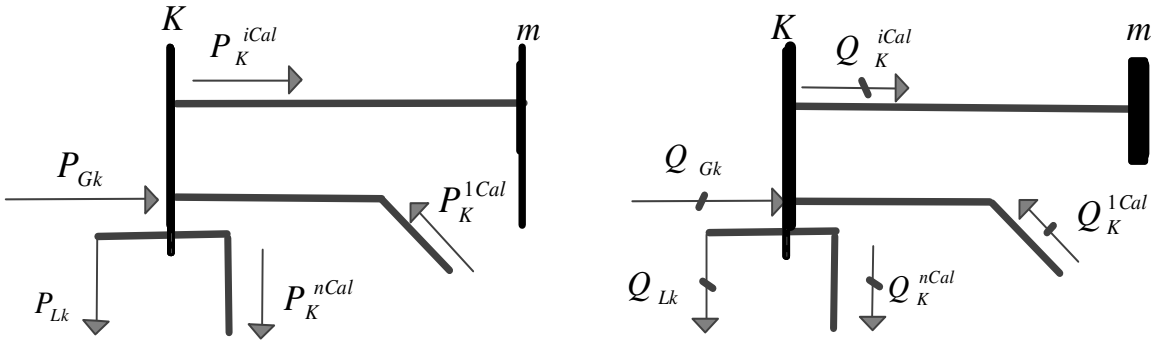

Figure 6: Power balance at bus K for active and reactive component

Where F represents the set of n nonlinear equations and X is the vector of n unknown state variables. The essence of the method consists of determining the vector of state variables X by performing a Taylors series expansion of F(X) about an initial estimate $X^{(0)}$;

$$F(X) = F(X^{(0)}) + J(X^{(0)})\,(X - X^{(0)}) + \text{higher order terms} \quad (23)$$

Where $J(X^{(0)})$ is a matrix of first-order partial derivatives of F(X) with respect to X, termed the Jacobian, evaluated at $X = X^{(0)}$. This expansion lends itself to a suitable formulation for calculating the vector of state variables X by assuming that $X^{(1)}$ is the value computed by the algorithm at iteration1 and that this value is sufficiently close to the initial estimate $X^{(0)}$. Based on this premise, all high-order derivative terms in (23) may be neglected. Hence,

$$\begin{bmatrix} F_1(X^{(1)}) \\ F_2(X^{(1)}) \\ \vdots \\ F_n(X^{(1)}) \end{bmatrix} \cong \begin{bmatrix} F_1(X^{(0)}) \\ F_2(X^{(0)}) \\ \vdots \\ F_n(X^{(0)}) \end{bmatrix} + \begin{bmatrix} \frac{\partial F_1(X)}{\partial X_1} & \frac{\partial F_1(X)}{\partial X_2} & \cdots & \frac{\partial F_1(X)}{\partial X_n} \\ \frac{\partial F_2(X)}{\partial X_1} & \frac{\partial F_2(X)}{\partial X_2} & \cdots & \frac{\partial F_2(X)}{\partial X_n} \\ \vdots & \vdots & \vdots & \vdots \\ \frac{\partial F_n(X)}{\partial X_1} & \frac{\partial F_n(X)}{\partial X_2} & \cdots & \frac{\partial F_n(X)}{\partial X_n} \end{bmatrix}_{X=X^{(0)}} \times \begin{bmatrix} X_1^{(1)} - X_1^{(0)} \\ X_2^{(1)} - X_2^{(0)} \\ \vdots \\ X_n^{(1)} - X_n^{(0)} \end{bmatrix} \quad (24)$$

In compact form, and generalizing the above expression for the case of iteration (i).

$$F(X^{(i)}) \approx F(X^{(i-1)}) + J(X^{(i-1)})\,(X^{(i)} - X^{(i-1)}) \quad (25)$$

Where i = 1, 2….. Furthermore, if it is assumed that $X^{(i)}$ is sufficiently close to the solution $X^{(*)}$ then $F(X^{i}) \approx F(X^{*}) = 0$, Hence, (25) changes to (26)

$$F(X^{(i-1)}) + J(X^{(i-1)})\,(X^{(i)} - X^{(i-1)}) = 0 \quad (26)$$

And solving for $X^{(i)}$ gives rise to (27).

$$X^{(i)} = X^{(i-1)} - J^{-1}(X^{(i-1)})\,F(X^{(i-1)}) \quad (27)$$

The iterative solution can be expressed as a function of the correction vector.

$$\Delta X^{(i)} = X^{(i)} - X^{(i-1)} \quad (28)$$

$$\Delta X^{(i)} = -J^{-1}(X^{(i-1)})F(X^{(i-1)}) \quad (29)$$

And the initial estimates are updated using the following relation:

$$X^{(i)} = X^{(i-1)} + \Delta X^{(i)} \quad (30)$$

The calculations are repeated as many times as required using the updated values of X in (30). This is done until the mismatches ΔX are within a prescribed small tolerance that is 1e-12. In order to apply the Newton-Raphson method to the power flow problem, the relevant equations must be expressed in the form of (30), where X represents the set of unknown nodal voltage magnitude and phase angles. The power mismatch equations ΔP and ΔQ are expanded around a base point $(\theta^{(0)}, V^{(0)})$ and hence, the power flow Newton-Raphson algorithm is expressed by (31).

$$\begin{bmatrix} \Delta P \\ \Delta Q \end{bmatrix}^{(i)} = -\begin{bmatrix} \frac{\partial P}{\partial \theta} & \frac{\partial P}{\partial V} V \\ \frac{\partial Q}{\partial \theta} & \frac{\partial Q}{\partial V} V \end{bmatrix}^{(i)} \begin{bmatrix} \Delta\theta \\ \frac{\Delta V}{V} \end{bmatrix}^{(i)} \quad (31)$$

The various matrices in the Jacobian may consist of (nb-1) X (nb-1) elements in (32).

$$\begin{cases} \frac{\partial P_K}{\partial \theta_M}, & \frac{\partial P_K}{\partial V_M} V_M, \\ \frac{\partial Q_K}{\partial \theta_M}, & \frac{\partial Q_K}{\partial V_M} V_{M,} \end{cases} \quad (32)$$

where K = 1,……nb, and m = 1,……nb, but omitting the slack bus entries.

3.3 Power flow model for the STATCOM (FACTS device)

Sequel to the discussion of the STATCOM operational characteristics, it is reasonable to expect that for the purpose of positive sequence power flow analysis the STATCOM will be well represented by a synchronous voltage source with maximum and minimum voltage limits. The synchronous voltage source represents the fundamental Fourier series component of the switched voltage waveform at the a.c converter terminal of the STATCOM. The bus at which the STATCOM is connected is represented as a PV bus, which may change to a PQ bus in the event of limits violation. In such a case, the generated or absorbed reactive power would correspond to the violated limit. Unlike the SVC, The STATCOM consists of one VSC and its associated shunt-connected transformer. It is the static counterpart of the rotating synchronous condenser but it generates or absorbs reactive power at a faster rate because no moving parts are involved. In

principle, it performs the same voltage regulation function as the SVC but in a more robust manner and its operation is not impaired by the presence of low voltages. The STATCOM is represented as a voltage source for the full range of operation, enabling a more robust voltage support mechanism. The STATCOM equivalent circuit shown in figure 7 is used to derive the mathematical model of the controller included in the power flow algorithms.

The power flow equations for the STATCOM are derived from first principle:

$$E_{VR} = V_{VR}(\cos\delta_{VR} + j\sin\delta_{VR}) \quad (33)$$

Based on the shunt connection shown in figure 7 above, the following may be written:

$$S_{VR} = V_{VR}I_{VR}^{*} = V_{VR}Y_{VR}^{*}(V_{VR}^{*} - V_{VK}^{*}) \quad (34)$$

From figure 7, (35) – (38) are obtained for the converter and bus K [11-12].

$$P_{VR} = V_{VR}^2G_{VR} + V_{VR}V_K[G_{VR}\cos(\delta_{VR} - \theta_K) + B_{VR}\sin(\delta_{VR} - \theta_K)] \quad (35)$$

$$Q_{VR} = -V_{VR}^2B_{VR} + V_{VR}V_K[G_{VR}\sin(\delta_{VR} - \theta_K) - B_{VR}\cos(\delta_{VR} - \theta_K)] \quad (36)$$

$$P_K = V_{VR}^2G_{VR} + V_KV_{VR}[G_{VR}\cos(\theta_K - \delta_{VR}) + B_{VR}\sin(\theta_K - \delta_{VR})] \quad (37)$$

$$Q_K = -V_K^2B_{VR} + V_KV_{VR}[G_{VR}\sin(\theta_K - \delta_{VR}) - B_{VR}\cos(\theta_K - \delta_{VR})] \quad (38)$$

Using these power equations, the linearised STATCOM models are derived from (39) – (55), where the voltage magnitude V_{VR} and phase angle δ_{VR} are taken to be the state variables.

$$\begin{bmatrix} \Delta P_K \\ \Delta Q_K \\ \Delta P_{VR} \\ \Delta Q_{VR} \end{bmatrix} = \begin{bmatrix} \frac{\partial P_K}{\partial \theta_K} & \frac{\partial P_K}{\partial V_K}V_K & \frac{\partial P_K}{\partial \delta_{VR}} & \frac{\partial P_K}{\partial V_{VR}}V_{VR} \\ \frac{\partial Q_K}{\partial \theta_K} & \frac{\partial Q_K}{\partial V_K}V_K & \frac{\partial Q_K}{\partial \delta_{VR}} & \frac{\partial Q_K}{\partial V_{VR}}V_{VR} \\ \frac{\partial P_{VR}}{\partial \theta_K} & \frac{\partial P_{VR}}{\partial V_K}V_K & \frac{\partial P_{VR}}{\partial \delta_{VR}} & \frac{\partial P_{VR}}{\partial V_{VR}}V_{VR} \\ \frac{\partial Q_{VR}}{\partial \theta_K} & \frac{\partial Q_{VR}}{\partial V_K}V_K & \frac{\partial Q_{VR}}{\partial \delta_{VR}} & \frac{\partial Q_{VR}}{\partial V_{VR}}V_{VR} \end{bmatrix} \begin{bmatrix} \Delta\theta_K \\ \frac{\Delta V_K}{V_K} \\ \Delta\delta_{VR} \\ \frac{\Delta V_{VR}}{V_{VR}} \end{bmatrix}$$

$$\frac{\partial P_K}{\partial \theta_K} = -Q_K - V_K^2G_{VR}, \quad (40)$$

$$\frac{\partial P_K}{\partial \delta_{VR}} = V_KV_{VR}[G_{VR}\sin(\theta_K - \delta_{VR}) - B_{VR}\cos(\theta_K - \delta_{VR})] \quad (41)$$

$$\frac{\partial P_{VR}}{\partial \delta_{VR}} = -Q_{VR} - V_{VR}^2B_{VR} \quad (42)$$

$$\frac{\partial P_{VR}}{\partial \theta_K} = V_{VR}V_K[G_{VR}\sin(\delta_{VR} - \theta_K) - B_{VR}\cos(\delta_{VR} - \theta_K)] \quad (43)$$

$$\frac{\partial P_K}{\partial V_K}V_K = P_K + V_K^2G_{VR} \quad (44)$$

$$\frac{\partial P_K}{\partial V_{VR}}V_{VR} = V_KV_{VR}[G_{VR}\cos(\theta_K - \delta_{VR}) + B_{VR}\sin(\theta_K - \delta_{VR})] \quad (45)$$

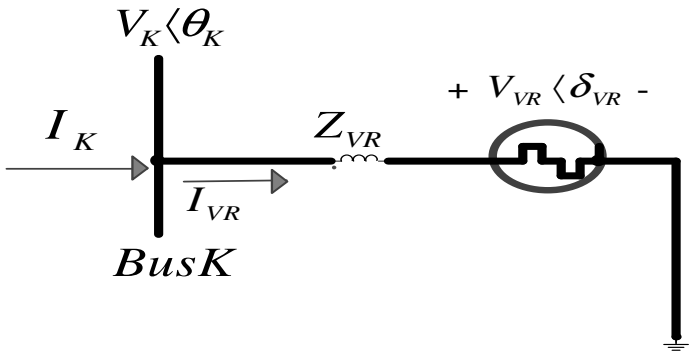

Figure 7: Static Compensator (STATCOM) equivalent circuit.

$$\frac{\partial P_{VR}}{\partial V_{VR}}V_{VR} = P_{VR} + V_{VR}^2G_{VR} \quad (46)$$

$$\frac{\partial P_{VR}}{\partial V_K}V_K = V_{VR}V_K[G_{VR}\cos(\delta_{VR} - \theta_K) + B_{VR}\sin(\delta_{VR} - \theta_K)] \quad (47)$$

$$\frac{\partial Q_K}{\partial \theta_K} = P_K - V_K^2 G_{VR}, \quad (48)$$

$$\frac{\partial Q_K}{\partial \delta_{VR}} = -V_K V_{VR}[G_{VR}\cos(\theta_K - \delta_{VR}) + B_{VR}\sin(\theta_K - \delta_{VR})] \quad (49)$$

$$\frac{\partial Q_{VR}}{\partial \delta_{VR}} = P_{VR} - V_{VR}^2 G_{VR} \quad (50)$$

$$\frac{\partial Q_{VR}}{\partial \theta_K} = -V_{VR} V_K[G_{VR}\cos(\delta_{VR} - \theta_K) + B_{VR}\sin(\delta_{VR} - \theta_K)] \quad (51)$$

$$\frac{\partial Q_K}{\partial V_K} V_K = Q_K - V_K^2 B_{VR} \quad (52)$$

$$\frac{\partial Q_K}{\partial V_{VR}} V_{VR} = V_K V_{VR}[G_{VR}\sin(\theta_K - \delta_{VR}) - B_{VR}\cos(\theta_K - \delta_{VR})] \quad (53)$$

$$\frac{\partial Q_{VR}}{\partial V_{VR}} V_{VR} = Q_{VR} - V_{VR}^2 B_{VR} \quad (54)$$

$$\frac{\partial Q_{VR}}{\partial V_K} V_K = -V_{VR} V_K[G_{VR}\sin(\delta_{VR} - \theta_K) - B_{VR}\cos(\delta_{VR} - \theta_K)] \quad (55)$$

The above analysis is summarized in the flow chart presented in figure 8

3.4 A case study

A case study of Ogui-Enugu thirteen bus radial distribution network is analyzed.

This network is selected from the Enugu Zonal Distribution network of Power Holding Company of Nigeria. The bus with constant voltage and zero phase angle is presumed as the slack bus since it is connected to the larger system with a relatively infinite supply of electrical power. The slack bus is usually bus 1. In the network understudy, bus (8) is a PV generator bus so that voltage could be kept constant as the load on the network changes. All other buses in the network are PQ load buses.

The single-line diagram of the thirteen-bus network with the line contingency control variables is shown in figure 9.

Table 1: line parameters of the 13-bus network.

bus-bus	line no	t_{lsend}	t_{lrec}	$t_{lresistance}$	$t_{lreactance}$
1-2	1	1	2	0.02	0.06
1-8	2	1	8	0.08	0.24
1-11	3	1	11	0.06	0.18
2-3	4	2	3	0.06	0.18
2-6	5	2	6	0.04	0.12
2-7	6	2	7	0.01	0.03
3-4	7	3	4	0.08	0.24
3-5	8	3	5	0.06	0.18
8-9	9	8	9	0.06	0.18
9-10	10	9	10	0.04	0.12
11-12	11	11	12	0.01	0.03
12-13	12	12	13	0.08	0.24

Source: PHCN Ogui-Enugu 33/11kv distribution line data sheet 2009.

Table 2: bus parameters of the 13-bus network

bus no:	bus type	voltage magnitude	phase angle
1	1	1.05	0
2	3	1	0
3	3	1	0
4	3	1	0
5	3	1	0
6	3	1	0
7	3	1	0
8	2	1	0
9	3	1	0
10	3	1	0
11	3	1	0
12	3	1	0
13	3	1	0

Source: PHCN Ogui-Enugu 33/11kv distribution line data sheet 2009.

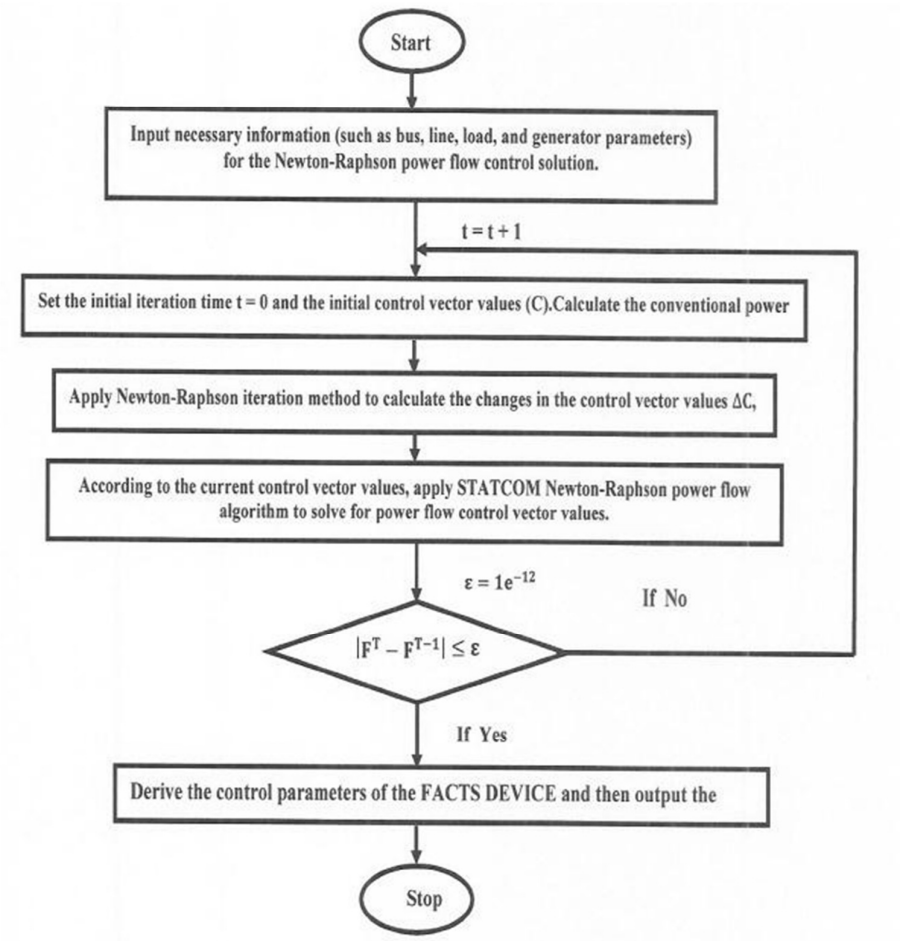

Figure 8: Flow chart of proposed flow control approach

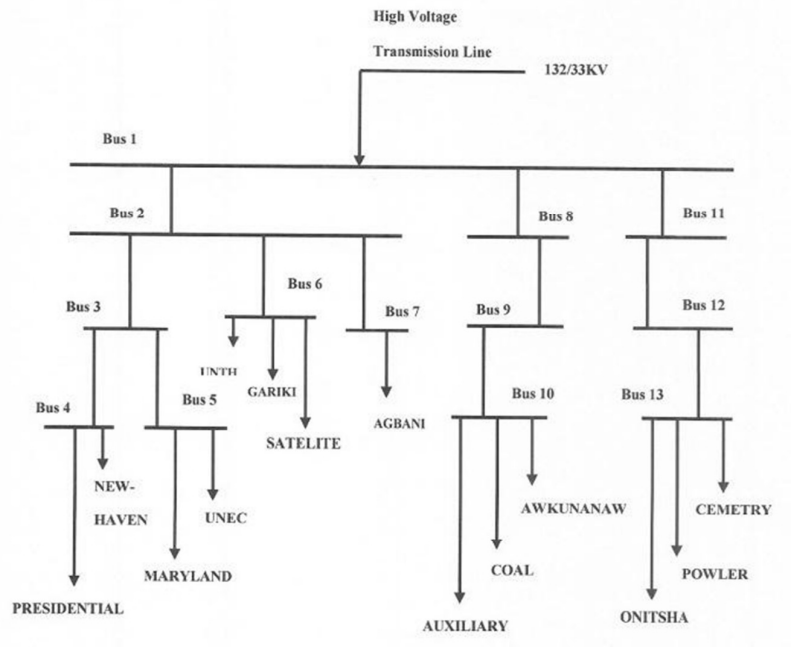

Figure 9: Thirteen bus radial network of Ogui-Enugu power distribution

Table 3: load data of the 13-bus network.

load bus	bus type	(without facts devices)		(with facts devices incorporated)	
		P(MW)	Q(MVar)	P(MW)	Q(MVar)
1	2	0.0298	0.0261	0.0000	0.0000
2	3	0.0297	0.0270	0.0000	0.0000
3	4	0.0247	0.0205	0.0000	0.0000
4	5	0.0258	0.0202	0.0000	0.0000
5	6	0.9257	0.0225	0.0000	0.0000
6	7	0.8273	0.0271	0.0000	0.0000
7	8	0.7680	0.0220	0.0000	0.0000
8	9	0.0279	0.0221	0.0000	0.0000
9	10	0.0266	0.0244	0.0000	0.0000
10	11	0.2995	0.0250	0.0000	0.0000
11	12	0.6989	0.0235	0.0000	0.0000
12	13	0.1878	0.0299	0.0000	0.0000

Source: PHCN Ogui-Enugu 33/11kv distribution line data sheet 2009.

Table 4: Generator data of the 13 bus network (ngn = 2)

Gen bus	bus no	Pgen	Qgen	Qmax	Qmin
1	1	0	0	+5	-5
2	8	0.4	0	+3	-3

4. Results and discussions of reslts.

In this section, the impact of connecting a static synchronous compensator STATCOM to a thirteen bus Ogui-Enugu distribution network is presented and analyzed. The STATCOM is connected to bus 13 of the Ogui-Enugu distribution network. The results of the analysis for the network without FACTS-DEVICES and the network with FACTS-DEVICE operating in the voltage range of $0.9 \leq x \leq 1.1$ were obtained. These results tabulated and plotted in this section were realized using Matlab power flow programs.

The comparative plots of voltage magnitude, voltage angle, real and reactive power of the network for conventional Newton-Raphson Power Flow and STATCOM Newton-Raphson Power flow are shown in figures 10, 11, 12 and 13 respectively.

From the plots shown above, it is significant to note that the STATCOM FACTS DEVICE increased the active power flow in buses 11 to 13 but conversely reduced the reactive power flow in those buses. This has improved the active power flow available in the power network for useful purposes. As the load demand on the supply system changes, the voltage at the consumer's terminal changes correspondingly. The variations of voltage at the consumer's terminals are undesirable and must be kept within prescribed limits of $\pm 6\%$ of the declared voltage. However, it was observed from the analysis of Ogui-Enugu Radial Power Distribution network that the voltages at buses 11 to 13 without STATCOM are not within the acceptable voltage magnitude limits as depicted in figure 4.2. The drop in voltage magnitude beyond the acceptable limits experienced by consumers is usually caused by increased load demand on the network made by consumers, power theft and technical losses. In this paper, voltage limit operating problem and power flow problem have been solved using STATCOM FACTS DEVICE to supply reactive power in order to maintain voltage magnitude constant in buses 11 to 13 and eventually made the bus voltages fall within the prescribed limits of $\pm 6\%$ of the declared voltage. Again the STATCOM FACTS DEVICE eminently increased the active power flow in buses 11 to 13 but conversely reduced the reactive power flow in those buses as shown in figures 12 and 13 respectively. The

STATCOM FACTS-DEVICE applied on this network thus, solved the problem of voltage variations at buses 11-13 by maintaining their values to 1.0 p.u. This also ensures regularization of voltage supply to incandescent lamps, smooth operation of the induction motor, a minimized heating effect of distribution transformers and improved energy efficiency of the power distribution networks.

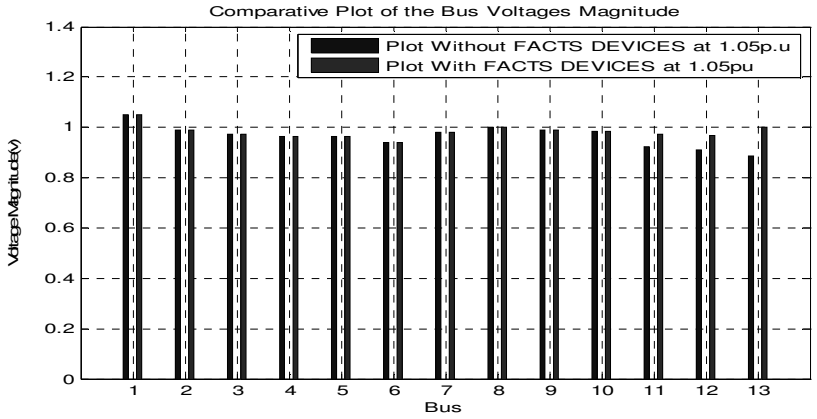

Figure 10: Comparative plot of the bus voltage magnitude

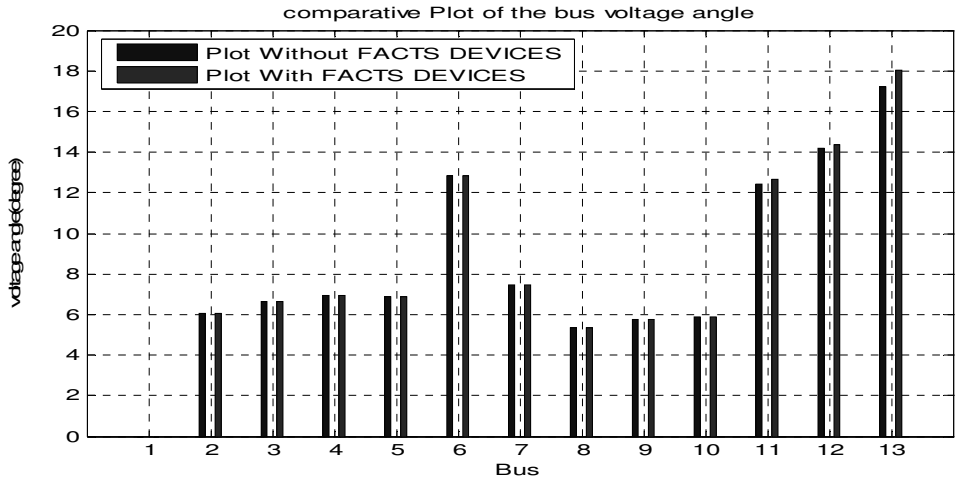

Figure 11: Comparative plot of the Absolute Values of The Network Bus Voltage Angles

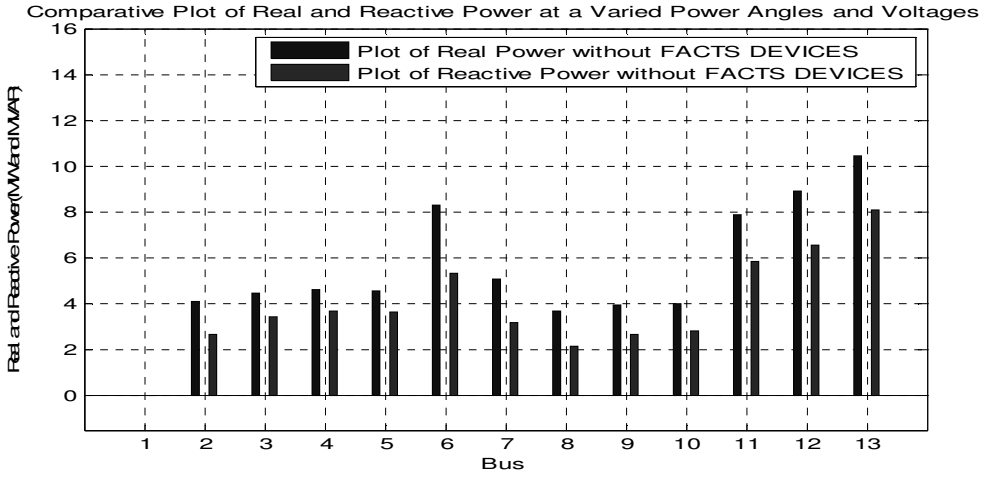

Figure 12: Comparative Plot of Real and Reactive Power Flow without STATCOM FACTS DEVICE

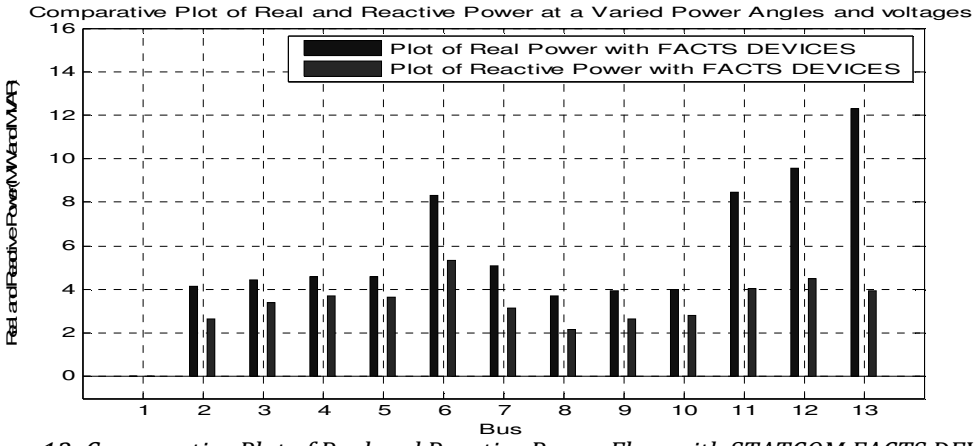

Figure 13: Comparative Plot of Real and Reactive Power Flow with STATCOM FACTS DEVICE

5. Conclusion

It is pertinent to state that for satisfactory operation of distribution networks, it is desirable that consumers are supplied with substantially constant voltage because too wide variations of voltage may cause erratic operation or even malfunctioning of industrial and consumers' appliances. In accordance with (2a) and (2b), the reactive power flow is determined mainly by the magnitude of the voltage source, V_S and the VSC output fundamental voltage V_{VR}. For $V_{VR} > V_S$, the VSC generates reactive power and consumes reactive power when $V_{VR} < V_S$. This voltage limit operating problem is usually solved by using STATCOM to supply reactive power in order to maintain voltage magnitude constant. From Ogui-Enugu power distribution network analysis result, $V_{VR} = 1.0238$ this implies that $V_{VR} > V_S$ which falls within the range of $V_{VRHI(1)} = 1.1$ *and* $V_{VRlo(1)} = 0.9$ as specified in the function SSC Data. The SSCPQsend result of 0+0.2380i shows that the VSC generates reactive power of 24Mvar in order to keep the voltage magnitude at 1p.u at bus 13 and improved the voltage profile at buses 11 and 12 respectively to almost 1p.u. Though the STATCOM VSC generated a reactive power of 24Mvar into the network, it is significant to note that the slack generator (bus 1) reduced its reactive power generation from 103Mvar to 77Mvar that is by 26Mvar (25%) as shown in Appendix 1. Again, from (2a) and (2b), the active power flow between the **a.c** source and the V_{SC} is controlled by the phase angleδ_{VR}. Active power flows into the VSC from the **a.c** source for lagging $\delta_{VR}(\delta_{VR} > 0)$and flows out of the VSC from the A.C source for leading $\delta_{VR}(\delta_{VR} < 0)$. From the Ogui-Enugu distribution network analysis, $T_{VR} = -18.0265$. Hence, increased active power flows out of the STATCOM VSC from the **a.c** source into the power network. This is eminently shown in buses 11, 12 and 13 in the comparative plot of Real and Reactive power flow with FACTS-DEVICE and without FACTS-DEVICE shown in Figures 12 and 13 respectively.

References

[1] Arrillaga, J. "High Voltage Direct Current Transmission", *Institute of Electrical Engineering Conference paper*, London, August, 1998, pp 36-46.

[2] Anya-Lara, O. and Acha, E. "Modeling and Analysis of Custom Power Systems by PSCAD/EMTDC". *IEEE Transactions on Power Delivery* Vol.7, No.1, Oct. 2002, pp.266-272.

[3] Larsen, E.V. Bowler, Damsky, C. and Nilson, B.S. "Benefits of Thyristor Controlled Series Compensation", *International Conference on Large High Voltage Electric System (CIGRE) paper*, Paris, Sept.1992, pp.38-40.

[4] Christl, N. Hedin, R. Sadek, K. Lutzelberger, P. Krause, P.E. Mc Kenna, S.M. Montoya, A.H. and Torgersen, D. "Advanced Series Compensation (ASC) with thyristor control impedance", *International conference on Large High Voltage Electric Systems (CIGRE)",* Paris, Sept. 1992, pp.38-50.

[5] Ambriz – Perez, H. Acha, E. and Fuerte-Esquivel, C.R. "Advanced SVC models For Newton-Raphson Load Flow and Newton Optimal Power flow studies", *IEEE Transactions on Power Systems*, Vol. 15 No.1, Nov. 2000, pp.129-136.

[6] Fuerte-Esquivel, C.R. and Acha, E. "Newton-Raphson Algorithm for the reliable solution of Large Power Networks with Embedded FACTS DEVICES", *IEE Proceedings on Generation, Transmission and Distribution*, Vol.143. No.5, Sept. 1996, pp.447-454.

[7] Peterson, N.M. and Scott Meyer, W. "Automatic Adjustment of Transformer and Phase Shifter Taps in the Newton Power Flow", *IEEE Transactions on Power Apparatus and Systems* PAS Vol. 90. No.1, Jan. 1974, pp.103–108.

[8] Scott, B. "Review of Load-Flow Calculation methods", *IEEE Proceedings*, Vol.62, No.6, July, 1974, pp.916-929.

[9] Scott, B. and Alsac, O. "Fast Decoupled Load Flow", *IEEE Transactions on Power Apparatus and Systems* PAS. Vol.93, No.2, Aug. 1978, pp.859-862.

[10]Tinney and Hart. C.E. "Power Flow Solution by Newton Method", *IEEE Transactions on Power Apparatus and Systems* PAS Vol.86. No.11, Nov. 1967, pp.1449-1460.

[11] Acha, E. Fuerte-Esquivel, C.R. Ambriz-Perez, H. and Angeles-Camacho, C. *FACTS Modeling and Simulation in Power Networks.* John Wiley and sons, New-York, 2004.

[12] Fuerte-Esquivel, C.R. and Acha, E. Newton-Raphson Algorithm for the reliable solution of Large Power Networks with Embedded FACTS DEVICES. *IEE Proceedings on Generation, Transmission and Distribution*, Vol.143. No.5, Sept. 1996, pp.447-454.

APPENDIX

Simulation result for pq bus power without facts device. PQBUSPOWER (Mw & Mvar)	Simulation result for pq bus power with facts device. PQBUSPOWER (Mw & Mvar)
3.7250 - 1.0292i	3.7175 - 0.7685i
-0.0298 + 0.0261i	-0.0298 + 0.0261i
-0.0297 + 0.0270i	-0.0297 + 0.0270i
-0.0247 + 0.0205i	-0.0247 + 0.0205i
-0.0258 + 0.0202i	-0.0258 + 0.0202i
-0.9257 + 0.0225i	-0.9257 + 0.0225i
-0.8273 + 0.0271i	-0.8273 + 0.0271i
0.4000 - 0.0212i	0.4000 - 0.0212i
-0.0279 + 0.0221i	-0.0279 + 0.0221i
-0.0266 + 0.0244i	-0.0266 + 0.0244i
-0.2995 + 0.0250i	-0.2995 + 0.0250i
-0.6989 + 0.0235i	-0.6989 + 0.0235i
-0.1878 + 0.0299i	-0.1878 - 0.2081i